

EVALUATION OF FORCES IN MANDIBULAR ELEVATOR MUSCLES FOR SELECTED LOAD CASES

P. Stróżyk, A. Szust

Faculty of Mechanical Engineering
Wrocław University of Technology
Wrocław 50-371, Łukasiewicza 5, Poland

e-mail: przemyslaw.strozyk@pwr.edu.pl, agnieszka.szust@pwr.edu.pl ; web page: <http://www.wm.pwr.wroc.pl>

Keywords: mandible, muscle, muscular forces, FEM

ABSTRACT: *A 3D mathematical model, consisting of three muscles (the masseter, the medial pterygoid muscle and the temporal muscle) and the mandible bone, was used to carry out a simulation in order to determine the values of the muscular forces as a function of the value of the bite forces and the place of their application on the dental arches. On the basis of experiments thirty five load cases were developed for the mandible. Classic methods of analytical statics and FEM were used to calculate the muscular forces. The assumption that the model is in a state of equilibrium and the mechanical properties of the muscles and the mandible bone are the same as those of a continuous, isotropic and homogenous material was one of the principal assumptions made. The calculations showed the masseter and the medial pterygoid muscle to be the strongest muscles and the temporal muscle to be the weakest muscle, regardless of the load case.*

1. INTRODUCTION

The mandible bone together with the skull and the muscular system form a complex kinematic system in which the mandible and the muscles can be regarded as mobile members fixed to the skull constituting an immobile base for them. A mechanical analysis usually covers the kinematics of such a system and the load equilibrium conditions for selected configurations as well as the deformability and strength of the components. At the stage of kinematic and static calculations the positions of the system (or its parts), in which loads reach the highest values, are determined. The active and passive forces are calculated using the classic methods of analytical statics. In order to solve the problem formulated above one should first specify: the number of muscles, the basic load configuration, the model support and the values of the active external forces generated by the muscle system.

The number of muscles (8–24 acc. to the literature) taken into account in mandible investigations depends on the complexity of the mathematical model and the aim of the investigation [1,2,3,4,5,6]. The load diagram is determined on the basis of a kinematic analysis of the temporomandibular joint (TMJ) in which the following movements: the hinge movement (the lowering and lifting of the mandible), the sliding movement (moving the mandible forward and backward) and the movement of mastication (being a combination of the two previously mentioned movements) are performed [7]. Two groups of muscles, i.e. the muscles lowering and lifting the mandible, are responsible for executing the movements [7]. Therefore one can assume that there exist at least two general load schemes (the lifting and lowering of the mandible) identical for all people, i.e. universal, since they are based on the same components (the support – TMJ, the active external forces – the muscular forces, the passive external forces – the support reactions, and the bite forces).

Considering that mainly the muscles which lift the mandible act during mastication, the next two load schemes, corresponding to the biting off and mastication of the morsel, are obtained. Each of the schemes can be modified (e.g. by changing the position of the support or the force application point) depending on the purpose of the calculations. If after the modification the general scheme is preserved, the new support and loading configuration becomes not a new loading scheme, but a load case.

One of the principal stages in the development of a loading scheme is the adoption of a model of the muscle action on the mandible bone. An analysis of the places of attachment of the muscles to the mandible bone indicates that the muscular forces can be distributed on surfaces or along lines. A single force vector is often used to model a single muscle [1,8] or a group of muscles [9,10]. Assuming that the model is planar (2D) one can construct a system consisting of at least three vectors: two vectors representing the reactions in temporomandibular joint (TMJ) and the bite forces, and a vector representing the muscles (e.g. the muscles lifting the mandible). In the case of a spatial (3D) model, one gets at least five vectors: two vectors representing the reactions in TMJ, one vector representing the bite forces and two vectors representing the group of muscles (the masseter, the medial pterygoid muscle and the temporal muscle) on both sides of the mandible.

In the next stage the forces generated by the particular muscles, depending on the adopted loading scheme, are determined. It is assumed that the muscular forces are proportional to the active physiological cross-section (PCS) [11,12] and the bioelectric activity (EMG) [13,14], and their values as a function of PCS are calculated from empirical equations [14,15,16].

In the literature on the subject one can find various load cases in both experimental studies [17,18] and numerical computations [19,20]. In view of strength calculations connected with, e.g., the examination and assessment of the union of bone fragments (fracture [21,22], Bilateral Sagittal Splint Osteotomy (BSSO) [23,24,25]), the optimization of plate implants [26,27] and the resection of the mandible bones [28]), load cases which take into account the anatomically and physiologically normal interaction between the muscles, the mandible and the skull should be used.

The main aim of this research was to determine the muscular forces as a function of two parameters: the bite force and its location on the dental arches, for 35 load cases.

Computations were carried out for two principal schemes, i.e. for biting off and mastication. Therefore only the muscles taking part in the lifting of the mandible (the masseter muscle, the temporal muscle and the medial pterygoid muscle) were taken into account and the computations were performed within rigid body mechanics, i.e. they were limited to solving the statics problem.

2. MATERIALS AND METHODS

2.1. General assumptions

The primary stage of the model studies consisted in adopting assumptions concerning, among other things, the load, the setting and fixing of the model and the mechanical properties of the mandible bone and the muscles. In order to determine the values of the forces generated by the mandibular elevator muscles [7] during static biting the following assumptions were adopted:

1. the model setting corresponded to the position in which the distance between the mandible and the maxilla amounted to 4 mm [12];
2. the active forces were the bite forces while the passive forces were the reactions in the places in which the model was fixed;
3. the calculations of the muscular forces took into account only the bite force components acting perpendicularly to the occlusion plane, i.e. component P_L and component P_R on respectively the left and right dental arch;
4. regardless of the load case, the algebraic sum of P_L and P_R was equal to the total bite force (P);
5. the lines of forces P_L , P_R and P were in one plane – referred to as the plane of loading (fig. 1);
6. the trace of the plane of loading passed through the pairs of corresponding teeth (fig. 2);
7. the value of P , corresponding to a given plane of loading (fig. 2), was always constant, regardless of the adopted load case (fig. 3); only the values of P_L and P_R and the location of line P (3) were variable; the general load cases (fig. 3a, b and c) were formulated on the basis of [20,29]; since the physical mandible model lacked symmetry, two additional cases were taken into account (fig. 3d and e);

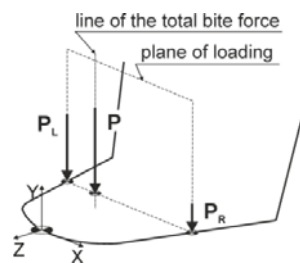


Fig. 1. Schematic showing locations of components P_L , P_R and P_T on plane of loading.

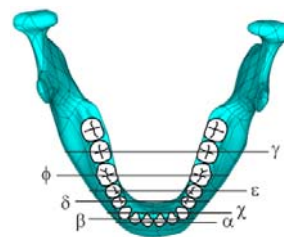


Fig. 2. Traces of planes of loading for pair of corresponding teeth.

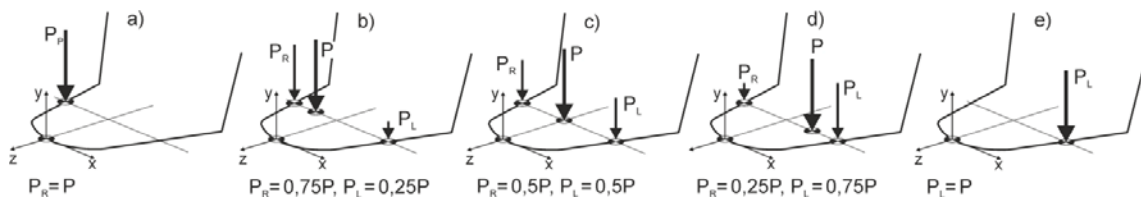


Fig. 3. General load cases used in computations: a) case I, b) case II, c) case III, d) case IV, e) case V. Ratios of P_L and P_R to P_T are specified for particular load cases.

8. all the load cases (fig. 3) were taken into account in planes β , χ , δ , ε , ϕ and γ , whereas in plane α only one case (fig. 3a) was taken into account;
 9. the computations were conducted for the equilibrium state: static biting [2,5,14,25,30];
 10. the head of the temporal joint did not change its position in the course of loading;
 11. the disc in the temporal joint, the articular capsule, the external and internal articular ligaments, the tendons, the deep part of the masseter muscle, and the lateral pterygoid muscle (because of its initial attachment some of the fibres are attached to the articular capsule and the disc) were not taken into account in the calculations [1,2,31];
 12. the particular muscles were modelled as a spatial set of inextensible tendons [3];
 13. the number of tendons depended on the particular muscle;
 14. a single tendon was a force vector while the set of tendons formed an arbitrary spatial force system.
- Since the computations were to be performed for static biting off and mastication, it was assumed that the computed values of the muscular forces would be instantaneous values closely connected with the actual position of the mandible (determined by the initial-value conditions and the boundary conditions), the load case and the mandible geometric dimensions.

2.2 Load (maximum bite forces)

Thirty five specific load cases (table 1), depending on the plane of loading (fig. 2) and the adopted system of forces (fig. 4), were prepared on the basis of the P values reported in [32]. Table 1 shows the load application place (the tooth number acc. to fig. 3) and the values of component bite forces P_L and P_R , depending on the load case.

Load case	Left dental arch		Right dental arch	
	Tooth number $^{\beta}$	P_L / $^{\beta}$ N	Tooth number $^{\beta}$	P_R / $^{\beta}$ N
I_{β}	-2	250 ₍₁₀₀₎	2	0
I_{χ}	-3	350 ₍₁₀₀₎	3	0
I_{δ}	-4	450 ₍₁₀₀₎	4	0
I_{ε}	-5	550 ₍₁₀₀₎	5	0
I_{ϕ}	-6	650 ₍₁₀₀₎	6	0
I_{γ}	-7	750 ₍₁₀₀₎	7	0
II_{β}	-2	187 ₍₇₅₎	2	63 ₍₂₅₎
II_{χ}	-3	262 ₍₇₅₎	3	88 ₍₂₅₎
II_{δ}	-4	337 ₍₇₅₎	4	113 ₍₂₅₎
II_{ε}	-5	412 ₍₇₅₎	5	138 ₍₂₅₎
II_{ϕ}	-6	487 ₍₇₅₎	6	163 ₍₂₅₎
II_{γ}	-7	562 ₍₇₅₎	7	188 ₍₂₅₎
III_{β}	-2	125 ₍₅₀₎	2	125 ₍₅₀₎
III_{χ}	-3	225 ₍₅₀₎	3	225 ₍₅₀₎
III_{δ}	-4	225 ₍₅₀₎	4	225 ₍₅₀₎
III_{ε}	-5	275 ₍₅₀₎	5	275 ₍₅₀₎
III_{ϕ}	-6	325 ₍₅₀₎	6	325 ₍₅₀₎
III_{γ}	-7	375 ₍₅₀₎	7	375 ₍₅₀₎

Load case	Left dental arch		Right dental arch	
	Tooth number $^{\beta}$	P_L / $^{\beta}$ N	Tooth number $^{\beta}$	P_R / $^{\beta}$ N
IV_{β}	-2	63 ₍₂₅₎	2	187 ₍₇₅₎
IV_{χ}	-3	88 ₍₂₅₎	3	262 ₍₇₅₎
IV_{δ}	-4	113 ₍₂₅₎	4	337 ₍₇₅₎
IV_{ε}	-5	138 ₍₂₅₎	5	412 ₍₇₅₎
IV_{ϕ}	-6	163 ₍₂₅₎	6	487 ₍₇₅₎
IV_{γ}	-7	188 ₍₂₅₎	7	562 ₍₇₅₎
V_{β}	-2	0	2	250 ₍₁₀₀₎
V_{χ}	-3	0	3	350 ₍₁₀₀₎
V_{δ}	-4	0	4	450 ₍₁₀₀₎
V_{ε}	-5	0	5	550 ₍₁₀₀₎
V_{ϕ}	-6	0	6	650 ₍₁₀₀₎
V_{γ}	-7	0	7	750 ₍₁₀₀₎
IV_{α}^{β}	-1	125 ₍₅₀₎	1	125 ₍₅₀₎

Table 1. Load cases, places of application of forces P_L and P_R and force values.

$^{\beta}$ – the percentage of the bite force (vertical components P_L and P_R) corresponding to a given load, $^{\beta}$ – the numbering of the teeth was based on a modified Zsigmondy system [33] (the symbol in the shape of the reversed letter L was removed and the sign “-” was added to the digits representing the teeth in the left dental arch.

$^{\beta}$ – in load case IV_{α} the load was applied to a point situated at the contact between tooth -1 and tooth 1,

2.3. Numerical model

The 3D numerical model consisted of two parts: the mandible bone and the muscles taking part in the lifting of the latter [7]. The initial geometric model of the mandible was constructed in the Geomagic program on the basis of the scans (Atos II made by GOM mbH, Germany) of a 3D polyurethane model of the human mandible

(Synbone). The final version of the geometric model was made in Ansys ver. 14.5 (Ansys, Inc., 2012, USA) In addition, two volumes, corresponding to respectively the cortical tissue and the cancellous tissue (the crown of the teeth was left remaining), were generated in the model.

In order to model the muscles as inextensible tendons the surface (its shape) on which the muscle joins the mandible bone, the way of mapping the surface of the terminal muscle attachment, the number tendons used to model a single muscle, the spatial location of the tendons relative to the mandible, etc., were defined.

The contours of the muscle-bone attachment surfaces (on the skull and on the mandible) were adopted according to the anatomical data [34]. Then points were marked on the surfaces and connected by tendons (fig. 4). The masseter was modelled by 20 tendons which were used to connect 18 points (5 on the skull and 13 on the mandible). Twelve tendons and fifteen points (3 on the skull and 12 on the mandible) were used to model the medial pterygoid muscle. The temporal muscle was defined by 4 tendons and 8 points (4 on the skull and 4 on the mandible).

The model was supported in points located on the articular surface of the mandible head and in points corresponding to the muscle attachments on the skull (fig. 4). Three degrees of freedom were obtained in each of the above points.

The numerical model of the mandible bone was divided into 46431 tetrahedral elements of the Solid185 type, i.e. the cortical bone and the cancellous bone were represented by respectively 40119 and 6212 elements. The numerical model of the muscles was divided into 986 Link180 elements.

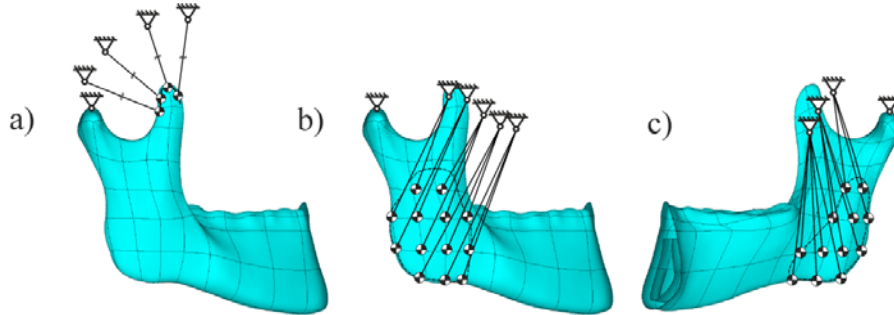


Fig. 4. Schematic showing location of tendons: a) temporal muscle, b) masseter, c) medial pterygoid muscle, and model support point. Dashed line marks place of attachment of muscle to mandible bone.

2.4 Mechanical properties of mandible and muscles

The mechanical properties: Young's modulus (E) and the Poisson ratio (ν), of the mandible bone (the cortical tissue and the cancellous tissue) were the same as those of a continuous, isotropic and homogenous material [19,35,36], and their values corresponded to the real bone tissue (table 2).

Yamada [37] and Fung [38] found that soft tissues are characterized by an exponential stress-strain relationship, but considering the aim of this study, a linear characteristic was used instead. Moreover, in the numerical model of the muscle it was assumed that the tendons modelling a single muscle had identical cross-sectional areas and the sum of the latter corresponded to the actual value of the physiological cross-sectional area (PCA) of the muscle (table 2).

		Bone ^[3,39,40]		Muscles of mastication		
		Cortical	Cancellous	Masseter	Temporal	Medial pterygoid
Young's modulus	E [MPa]	$1.7 \cdot 10^4$	$1.1 \cdot 10^4$	0.8 ^[41]		
Poisson ratio	ν	0.3	0.3	0.4 ^[42]		
Physiological cross-sectional area ^[12,43,44,45]	PCA [cm ²]	–	–	8.0	9.1	4.5

Table 2. Mechanical properties of cortical bone, cancellous bone and muscles, and values of cross-sectional area of single muscle.

3. RESULTS

The values of muscular forces S_R , as a function of the bite forces and the places of their application to the dental arches, were numerically calculated.

In order to calculate muscular forces S_R it was necessary to reduce the system of forces since it was found that:

- the spatial system of forces represented by the set of tendons (fig. 4) could be replaced by a single principal vector (S) and a pair of vectors with a moment (M) equal to the principal moment of all the forces relative to the adopted centre of reduction,
- the angle ($\alpha \pm SD$) between vectors S and M , for all the muscles, regardless of the load case, amounted to $\alpha_{SM} = 90.1^\circ \pm 0.5$; $\alpha_{SM} = 90^\circ$ was assumed for further analyses.

If $S \neq 0$, $M \neq 0$ and $\alpha_{SM} = 90^\circ$ (a special case of the reduction of any spatial system of forces), the system of forces comes down to the resultant force, i.e. S_R .

The so-called centres of reduction (BP) and local coordinate systems (with the origin in BP) were introduced individually for each muscle (fig. 5) in order to perform the reduction. In the case of the masseter and the medial pterygoid muscle, a common BP with one coordinate system (on account of the terminal attachment) was adopted, but the reduction was carried out individually for each of the muscles.

Reductions for the particular muscles were performed in accordance with the assumptions of statics. The values and spatial positions of vectors (direction cosines) of S and M and angle α_{SM} were determined using the classic equations of statics.

Since the absolute value, direction and sense of vector S_R (table 3) and the inclination angles (table 4) are the same as S ($|S_R| = |S|$), in order to spatially determine the position of S_R for the particular muscles the line of the vector (fig. 6) and distance h (table 5) at which vector S_R should be located so that when multiplied by this distance it would be equal to absolute value M had to be determined. Considering that $\cos(S, M) = 90^\circ$, h was determined from equation 1 while the force line location (for the adopted boundary and initial conditions) was determined using analytical geometry.

$$h = \frac{|M|}{|S|} \quad (1)$$

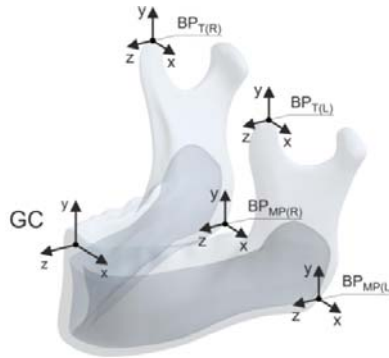


Fig. 5. Position of local coordinate systems and reduction centres SR relative to global coordinate system GC; BP_{T(L)} and BP_{T(R)} – reduction centre for temporalis muscle on respectively left and right side, BP_{MP(L)} and BP_{MP(R)} – reduction centre for masseter and medial pterygoid muscle on respectively left and right side, GC – global coordinate system (system origin is located between incisors).

Load case	Left side			Right side		
	S _{RM}	S _{RP}	S _{RT}	S _{RM}	S _{RP}	S _{RT}
I _β	175	67	41	134	66	29
I _χ	263	95	59	168	87	39
I _δ	326	128	73	201	106	46
I _ε	356	171	86	195	109	45
I _φ	384	218	101	177	103	42
I _γ	370	281	114	136	81	33
II _β	166	65	39	143	68	30
II _χ	241	91	56	190	92	41
II _δ	294	119	69	230	115	50
II _ε	319	154	78	234	129	52
II _φ	336	189	88	226	139	52
II _γ	315	231	97	188	141	48
III _β	157	63	38	151	71	32
III _χ	220	87	53	210	98	44
III _δ	264	111	64	261	125	54
III _ε	281	138	69	271	150	59
III _φ	289	161	76	273	175	63
III _γ	262	183	78	240	201	65
IV _β	148	61	37	160	73	33
IV _χ	198	83	50	230	103	46
IV _δ	232	103	59	291	134	58
IV _ε	242	120	63	309	170	66
IV _φ	241	132	63	319	210	75
IV _γ	209	135	60	292	263	82
V _β	139	59	36	169	75	34
V _χ	177	79	47	250	108	49
V _δ	201	94	55	320	143	63
V _ε	204	103	56	346	190	74
V _φ	192	103	53	366	246	87
V _γ	155	87	43	344	325	98
VI _β	161	64	39	155	71	32

Table 3. Values (rounded to 1N) of muscular forces S_{RT}, S_{RM}, S_{RP} N; S_{RM} – masseter, S_{RP} – medial pterygoid muscle, S_{RT} – temporal muscle.

Muscles of mastication	Side	h ± SD [mm]	
Masseter	right	h _{Mr}	17.0±0.0
	left	h _{Ml}	17.0±0.0
Temporal	right	h _{Tr}	13.0±4.3
	left	h _{Tl}	14.0±4.7
Medial pterygoid	right	h _{Pr}	16.0±1.0
	left	h _{Pl}	17.0±1.0

Table 5. Mean value of vector h for selected muscles.

Load Case	Left side			Right side		
	m	n	k	m	n	k
I _{β-VI_β}	S _{RM}			S _{RM}		
	99	23	67	82	24	68
I _{β-VI_β}	S _{RP}			S _{RP}		
	67	23	88	113	23	87
I _{β-VI_β}	S _{RT}			S _{RT}		
	I _β	108	50	135	75	51
I _χ	108	50	135	75	51	137
I _δ	108	50	134	75	51	137
I _ε	108	46	131	75	51	137
I _φ	107	42	126	75	51	137
I _γ	107	36	121	75	50	137
II _β	108	50	135	75	50	137
II _χ	108	50	135	75	50	136
II _δ	108	50	135	75	50	137
II _ε	108	47	132	75	50	136
II _φ	107	43	128	75	50	136
II _γ	107	37	122	75	47	133
III _β	108	50	135	75	50	136
III _χ	108	50	135	75	50	136
III _δ	108	50	135	75	50	136
III _ε	108	49	134	75	50	136
III _φ	108	46	131	75	47	134
III _γ	107	40	125	76	43	129
IV _β	108	50	135	75	50	136
IV _χ	108	50	135	75	50	136
IV _δ	108	50	135	75	50	136
IV _ε	108	50	135	75	48	134
IV _φ	108	49	134	76	45	131
IV _γ	107	44	129	76	41	127
V _β	108	50	135	75	50	136
V _χ	108	50	135	75	50	136
V _δ	108	50	135	75	49	136
V _ε	108	50	135	75	46	133
V _φ	108	50	135	76	43	130
V _γ	108	50	135	76	39	126
VI _β	108	50	135	75	50	137

Table 4. Values (rounded to 1°) of inclination angles¹ of m, n and k, S_{RM} – masseter, S_{RP} – medial pterygoid muscle, S_{RT} – temporal muscle.

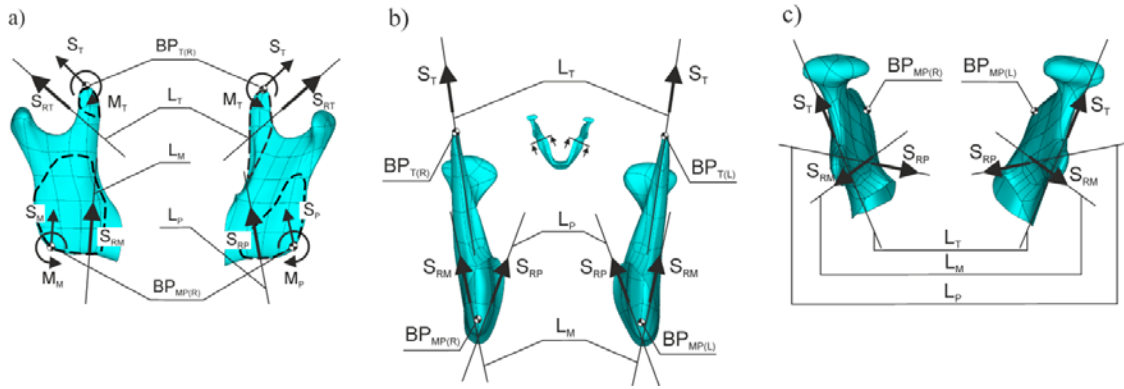


Fig. 6. Spatial scheme showing position of line of vectors S_{RT} , S_{RM} , S_{RP} relative to adopted reduction centres: a) buccal and lingual view – right ramus, b) frontal view – right and left ramus, c) mandibular occlusal view – right and left ramus; Scheme drawn using vector h values given in table 5; $BP_{T(R)}$, $BP_{T(L)}$ – see fig. 5, S_T , S_M , S_P – principal vector for respectively temporal muscle, masseter and medial pterygoid; M_T , M_M , M_P – moment of principal vector for respectively temporal muscle, masseter and medial pterygoid muscle; S_{RT} , S_{RM} , S_{RP} – resultant vector for respectively temporal muscle, masseter and medial pterygoid muscle, L_T , L_M , L_P – line of resultant vector for temporal muscle, masseter and medial pterygoid muscle.

4. DISCUSSION

The system of forces (the set of tendons for the particular muscles is an arbitrary spatial system of forces) was subjected to reduction in order to determine the muscular forces in the masseter, the medial pterygoid muscle and the temporal muscle. The systems for the individual muscles reduced themselves to two perpendicular vectors S and M , which were further reduced to a single vector: so-called resultant force S_R . The modulus, direction and sense of S_R are the same as those of vector S , i.e. $|S_R|=|S|$ and its line is shifted parallel to S by value h . Therefore it was assumed that the muscular forces would be represented by vectors S_{RT} , S_{RM} , S_{RP} .

Numerical computations showed that the values of S_{RT} , S_{RM} and S_{RP} change as indicated by the results obtained for simple mechanical systems, e.g. a beam supported at one of its ends and suspended from a bar element, loaded with concentrated force P which moves towards the support and its value increases at the same time. One should note that the maximum force values for the masseter (S_{RM}) and the temporal muscle (S_{RT}) do not correspond to the greatest force P . On the working side the maximum value of S_{RM} occurs at $P = 650N$ (the load on the first molar tooth) while on the balancing side it occurs at $P = 550N$ (the load on the second premolar tooth) for an asymmetric load, and at $P = 650N$ for a symmetric load. The maximum force in the medial pterygoid muscle (S_{RP}) corresponds to $P = 750N$, on both the working side and the balancing side, except for case I_β , in which the maximum value of S_{RP} for the balancing side corresponds to $P_T = 550N$. This behaviour is not something obvious, but it turns out that a similar effect can be observed in simple mechanical systems (see the example given above) provided $P_{(max)}/P_{(min)} \geq 1.75$ (verification was carried out only up to 3.5 since in the present study $P_{T(max)}/P_{T(min)}=3$).

In the literature on the subject the values of muscular forces are reported for both the whole muscle [2,8,12,43,44,46,47] and the muscle divided into several areas [6,14,48,49,50]. Only the forces for the whole muscle were analyzed in the present study. As regards their quality, the results (table 3) are closest to the ones reported by Choi [47] who would load simultaneously the second premolar tooth and the first molar tooth, symmetrically to the medial plane. There is a clear similarity in the case of the masseter and the medial pterygoid muscle, but the results obtained by the present authors for the temporal muscle are 5.6–6.2 times lower than the ones reported by Choi [47].

The position of a vector in space can be determined using, e.g. direction cosines. Therefore, as part of this study it was also checked whether the angles for S_{RM} , S_{RP} and S_{RT} were functions of the load cases since Reina et al. [20], Korióth et al. [51] and Osborn [5] had adopted a 3D model and, despite the different cases of (symmetrically and asymmetrically) loading the mandible with bite forces, used constant inclination angles. The analysis showed that the comparison of the m , n and k values with the ones obtained by the above authors was imprecise due to the differences between the models and in the division of the muscle into areas (no division of the muscle into areas was used in the present study). Despite the differences, verification was carried out on the basis of [20,51], but only for the masseter and the medial pterygoid muscle. The m , n and k values were found to be comparable while the differences for the masseter and the medial pterygoid muscle amounted to respectively $\Delta m = \pm 4^\circ$, $\Delta n = \pm 3^\circ$, $\Delta k = \pm 5^\circ$ and $\Delta m = \pm 19^\circ$, $\Delta n = \pm 7^\circ$, $\Delta k = \pm 15^\circ$, for the left and right side.

In [2,4,14] it is stated that the line of vector S_{RT} , S_{RM} and S_{RP} should pass through the geometric centre of the surface area of the attachment of the muscle to the mandible bone. The fact that the above assumption was made

indicates that the muscle tension in the active physiological cross section (PCA) is uniform – all the muscle fibres are tensioned to the same degree. Whereas in [5] it is reported that muscle tension begins in the fibres most distant from the point of support and gradually appears in the successive fibres. The present authors did not find (had no access to) any data which would explicitly show what the distribution of the tension of the muscle fibres in the muscle cross section is. Therefore it was assumed that the line of vectors S_{RT} , S_{RM} and S_{RP} would not be the initial condition of the problem, but the result of calculations. Hence it was assumed that the arrangement of the tendons (each of the tendons being a force vector) corresponded to any spatial system of forces.

An analysis of the spatial position of lines L_T , L_M , L_P of the particular vectors S_{RT} , S_{RM} , S_{RP} (fig. 6) indicates that the direction of the moment of vector S_{RT} , S_{RM} and S_{RP} , relative to $BP_{T(R)}$, $BP_{T(R)}$ is consistent with the direction of M_T , M_M and M_P . The lines of vectors S_{RM} and S_{RP} are shifted (table 5) forward relative to the reduction centre while the line of vector S_{RT} is shifted (table 5) towards the mandible bone head. It is interesting that the h values of L_M and L_P are almost identical (table 5) and constant, regardless of the load case, and the magnitude of the shift of line L_P varies widely (table 5) depending on the load case since the values of the direction cosines also depend on the load case (table 4).

According to the literature reports, the muscular force is proportional to PCS [11,12] or EMG [13,14], whereas the present authors on the basis of the obtained results and the osteo-muscular anatomy [34] noticed that the two strongest muscles (table 3) have a larger attachment to the mandible bone (A_M) and the smallest attachment to the skull bone (A_S). Whereas the weakest muscle has the lowest A_M value, but a higher A_S value (table 6). To the authors' knowledge there have been no studies in which test and/or calculation results would relate the muscular force value to the size of muscle attachments. In order to explain the dependence between the muscle force and the size of the muscle attachment additional investigations need to be carried out to explicitly determine whether the results change if the temporal muscle is divided into an anterior part, a middle and a posterior part and whether this is the rule in the muscular system.

Muscles of mastication	Surface area of muscle attachment $1 \cdot 10^3 \text{ m}^2$	
	Mandible A_M ¹	Skull A_S ¹
Masseter	$1.2 \cdot 10^{-3}$	$0.2 \cdot 10^{-3}$
Temporal	$0.5 \cdot 10^{-3}$	$9.0 \cdot 10^{-3}$
Medial pterygoid	$0.4 \cdot 10^{-3}$	$0.1 \cdot 10^{-3}$

Table. 6. A_M and A_S values for masseter, medial pterygoid muscle and temporal muscle.

¹ The A_M and A_S values were determined on basis of the anatomical atlas [34].

At the current stage in the computations it is difficult to verify the assumptions and the model due to the fact there is no single biomechanical standard to which one could refer. Only individual cases can be verified or the computations can be carried using another model, e.g. one can change the arrangement of the tendons for the masseter and the medial pterygoid muscle to a parallel one and compare the results. This would require separate computations, which fall out of the scope of this paper.

5. CONCLUSIONS

1. The strongest muscles are the masseter and the medial pterygoid muscle and the weakest muscle is the temporal muscle.
2. Muscular forces S_{RM} , S_{RP} and S_{RT} depend on the load case.
3. The highest values of S_{RM} , S_{RP} and S_{RT} are generated on the working side during unilateral mastication, especially with the premolar and molar teeth, while the lowest values are generated when the food is being bitten off with the incisors, both on the left and right side.
4. Vertical components S_{RM_y} , S_{RP_y} and S_{RT_y} and horizontal components: S_{RM_z} , S_{RP_z} and S_{RT_z} for the masseter and the temporal muscle and S_{RM_x} , S_{RP_x} and S_{RT_x} for the medial pterygoid muscle have the greatest influence on the values of S_{RM} , S_{RP} and S_{RT} .
5. Inclination angles m , n , k and lines L_M , L_P of vectors S_{RM} and S_{RP} are constant and do not depend on the load case.
6. Inclination angles n and k of vector S_{RT} are variable and depend on the load case, whereas m is constant in the whole load range. The calculation results indicate that for a fixed mandible position, but at different bite force values and at different points of their application, the change in the position of vector S_{RT} is connected with the uneven tension in PCA. Thus one can advance the thesis that line L_T of vector S_{RT} for the fixed mandible position depends on the values of the bite force, but mainly on the places of their application to the dental arches.

In order to use the determined values of the muscular forces the model should be verified and checked whether it is a linear geometric system since only then it will be possible to rescale the muscular forces to the lower bite force values occurring during the biting off and mastication of food.

6. REFERENCES

1. Tuijt M., Koolstra J.H., Lobbezoo F., Naeije M., (2010), "Differences in loading of the temporomandibular joint during opening and closing of the jaw," *J. Biomechanics*, Vol. 43, 1048–1054
2. Koolstra J.H., van Eijden T.M.G.J., Weijs W.A., Naeije M., (1988), "A three-dimensional mathematical model of the human masticatory system predicting maximum possible bite forces," *J. Biomechanics*, Vol. 21, 563–576
3. Koolstra J.H., van Eijden T.M.G.J., (2005), "Combined finite-element and rigid-body analysis of human jaw joint dynamics," *J. Biomechanics*, Vol. 38, 2431–2439
4. Barbenel J. C., (1972), "The biomechanics of the temporomandibular joint: A theoretical study," *J. Biomechanics*, Vol. 5, 251–256
5. Osborn J. W., Baragar F. A., (1985), "Predicted pattern of human muscle activity during clenching derived from a computer assisted model: symmetric vertical bite forces," *J. Biomechanics*, Vol. 18, 599–612
6. van Essen, N.L., I.A. Anderson, I.A., P.J. Hunter, P.J., Carman, J.B., Clarke, R.D., Pullan, A.J., (2005), "Anatomically based modelling of the human skull and jaw," *Cells Tissues Organs*, Vol. 180, 44–53
7. Walocha J., Skawina A. (Editor), Gorczyca J., Skrzat J., (2006), *Szyja i głowa*, Jagiellonian University Press, Kraków
8. Kashi A., Roy Chowdhury A. Roy, Saha S., (2010), "Finite element analysis of a TMJ implant," *J Dent Res*. Vol. 89, 241–245
9. Armstrong J. E. A., Lapointe H. J., Hogg N. J. V., Kwok A. D., (2001), "Preliminary investigation of the biomechanics of internal fixation of sagittal split osteotomies with miniplates using a newly designed in vitro testing model," *J. Oral Maxillofac Surg.*, Vol. 59, 191–195.
10. Smith, R.J., (1978) Mandibular biomechanics and temporomandibular joint function in primates., Vol. 49, 341–350
11. Radu M., Marandici M., Hottel T.L., (2004), "The effect of clenching on condylar position: A vector analysis model," *Prosthet Dent.*, Vol. 91, 171–179
12. May B., Saha S., Saltzman M., (2001), "A three-dimensional mathematical model of temporomandibular joint loading," *Clinical Biomechanics*, Vol. 16, 489–495
13. Hof A.L., (1997), *The relationship between electromyogram and muscle force*, Sportverletz Sportschaden, 11,79-86
14. Pruijm G.J., De Jongh H.J., Ten Bosch J.J., (1980), "Forces acting on the mandible during bilateral static bite at different bite force levels," *J. Biomechanics*, Vol. 13, 755–763
15. Faulkner M., Hatcher D., Hay A., (1987), "A three-dimensional investigation of temporomandibular joint loading," *J. Biomechanics*, Vol. 20, 997–1002
16. Itoh K., Hayashi T., Miyakawa M., (1997), "Controllability of temporomandibular joint loading by coordinative activities of masticatory muscles: a two-dimensional static analysis," *Front Med Biol Eng.*, Vol. 8, 123–138
17. Ramos A., Ballu A., Mesnard M., Talaia P., (2011), "Numerical and experimental models of the mandible," *Exp. Mech.*, Vol. 51, 1053–1059
18. Meyer Ch., Kahn J.L., Lambert A., Boutemy P., Wilk A., (2000), "Development of a static simulator of the mandible," *J. Cranio Maxillofac Surg.*, Vol. 28, 278–286
19. Ichim I., Kieser J.A., Swain M.V., (2007), "Functional significance of strain distribution in the human mandible under masticatory load," *Numerical predictions. Arch Oral Bol.*, Vol. 52, 465–473
20. Reina J.M., Garcia-Aznar J.M., Dominguez J., Doblaré M., (2007), "Numerical estimation of bone density and elastic constants distribution in a human mandible." *J. Biomechanics*, Vol. 40, 826–836
21. Korkmaz H.H., (2007), "Evaluation of different miniplates in fixation of fractured human mandible with the finite element method," *Oral Surg, Oral Med, Oral Pathol, Oral Radiol and Endod*, Vol. 103:e1–e13
22. Ribeiro-Junior P.D., Magro-Filho O., Shastri K.A., Papageorge, M.B., (2010), "In vitro evaluation of conventional and locking miniplate/screw systems for the treatment of mandibular angle fractures," *Int. J. Oral Maxillofac. Surg.*, Vol. 39, 1109–1114.
23. Cheng-Jen Chuong Ch.J., Borotikar B., Schwartz-Dabney C., Sinn D.P., (2005), "Mechanical characteristics of the mandible after bilateral sagittal split ramus osteotomy: Comparing 2 different fixation techniques." *J. Oral Maxillofac Surg.*, Vol. 63, 68–76
24. Oguz Y., Uckan S., Ozden A.U., Uckan E., Eser A., (2009), "Stability of locking and conventional 2.0-mm miniplate/screw systems after sagittal split ramus osteotomy: finite element analysis." *Oral Surg, Oral Med, Oral Pathol, Oral Radiol and Endod.*, Vol. 108, 174–177
25. Stróżyk P., Nowak R., (2011), "Zastosowanie metody elementów skończonych do analizy stabilności zespołów stosowanych przy strzałkowej osteotomii gałęzi żuchwy," *Dent. Med. Probl.*, Vol. 48, 157–164
26. Lovald S.T., Wagner J.D., Baack B., (2009), "Biomechanical optimization of bone plates used in rigid fixation of mandibular fractures," *J. Oral Maxillofac Surg.*, Vol. 67, 973–985

27. Maurer P., Knoll W.D., Schubert J., (2003), "Comparative evaluation of two osteosynthesis methods on stability following sagittal split ramus osteotomy," *J. Cranio Maxillofac Surg.*, Vol. 31, 284–289
28. Jankowski L., Stróżyk P., Szust A., (2012), „Doświadczalna i numeryczna analiza deformacji zuchwy po częściowej resekcji,” *XXV Sympozjum Mechaniki Eksperymentalnej Ciała Stałego imienia prof. Jacka Stupnickiego*, Jachranka, 17–20.10., PW, s. 44–45, Warszawa
29. Manns A., Díaz G., (1988), *Sistema Estomatognático*, Sociedad Gráfica Almagro Ltda., Santiago de Chile.
30. Nickel J.C., Iwasaki L.R., Walker R.D., McLachlan K.R., McCall W.D. Jr., (2003), "Human Masticatory Muscle Forces during Static Biting," *J. Dent Res.*, Vol. 82, 212–217
31. Aleksandrowicz R., Ciszek B., (2007), *Anatomia kliniczna głowy i szyi*, Wydawnictwo Lekarskie PZWL, Warszawa
32. Chladek W., (2000), *Systemy modelowania wybranych stanów mechanicznych zuchwy ludzkiej*, Zeszyty Naukowe Politechniki śląskiej, Gliwice
33. <http://www.americantooth.com>
34. Sinelnikov, R., D., (1988), *Atlas of human anatomy*, MIR, Moscow
35. Ciftici Y., Canay S., (2000), "The effect of veneering materials on stress distribution in implant-supported fixed prosthetic restorations," *Int. J. Oral Maxillofac Implants.*, Vol. 15, 571–582
36. Gallas M., Fernández J.R., (2004), "A three-dimensional computer model of the human mandible in two simulated standard trauma situations," *J. Cranio Maxillofac Surg.*, Vol. 32, 303–307
37. Yamada H. (1970), *Strength of Biological Materials*, The Williams & Wilkins Company, Baltimore
38. Fung Y. C., (1993), *Biomechanics: mechanical properties of living tissues*, Springer-Verlag, New York
39. Nagasao T., Kobayashi M., Tsuchiya Y., Kaneko T., Nakajima T., (2003), "Finite element analysis of the stresses around fixtures in various reconstructed mandibular models – Part II (effect of horizontal load)," *J. Cranio Maxillofac Surg.*, 31, 168–175
40. Kimura A., Nagasao T., Kaneko T., Tamaki T., Miyamoto J., Nakajima T., (2006), "Adequate fixation of plates for stability during mandibular reconstruction," *J. Oral Maxillofac Surg.*, Vol. 34 193–200
41. Gross M.D., Arbel G., Hershkovitz I., (2001), "Three-dimensional finite element analysis of the facial skeleton on simulated occlusal loading," *J. Oral Rehabil.*, Vol. 28, 684–694
42. Choi A. P. Ch., (2008), *Estimation of Young's Modulus and Poisson's Ratio of soft tissue using indentation*, The Master of Philosophy, The Hong Kong Polytechnic University
43. Koolstra J.H., van Eijden T.M.G.J., (1992), "Application and validation of a three-dimensional mathematical model of the human masticatory system in vivo," *J. Biomechanics*, Vol. 25, 175–187
44. Pileickiene G., Surna A., Barauskas R., Surna R., Basevicius A., (2007), "Finite element analysis of stress in the maxillary and mandibular dental arches and TMJ articular disc during clenching into maximum intercuspatation, anterior and unilateral posteriori occlusion." *Stomatologia. Baltic Dental and Maxillofacial J.*, Vol. 9, 121–128
45. van Eijden T.M.G.J., Korfage J.A.M., Brugman P., (1997), "Architecture of the human jaw-closing and jaw-opening muscle," *Anat. Rec.*, Vol. 248, 464–474
46. Schumacher G.H., (1961), *Functionelle Morphologie der Kaumuskulatur*, VEB Gustav Fischer Verlag: Jena
47. Choi A.H., Ben-Nissan B., Conway R.C., (2005), "Three-dimensional modelling and finite element analysis of the human mandible during clenching," *Aust Dent J.*, Vol. 50, 42–48
48. Koolstra J. H. and van Eijden T. M. G. J., (2006), "Prediction of volumetric strain in the human temporomandibular joint cartilage during jaw movement," *J. Anat.*, Vol. 209, 369–380
49. Carlsöö S., (1952), "Nervous co-ordination and mechanical function of the mandibular elevators; an electromyographic study of the activity, and an anatomic analysis of the mechanics of the muscles," *Acta Odont Scand*, Supp Vol. 10, 1–132
50. Carlsöö S., (1958), "Motor units and action potentials in masticatory muscles; an electromyographic study of the form and duration of the action potentials and an anatomic study of the size of the motor units," *Acta Morph Neerl Scand*, Vol. 2, 13–19
51. Korioto T.W.P. and Hannam A.G., (1994), "Deformation of the Human Mandible During Simulated Tooth Clenching," *J. Dent Res.*, Vol. 73, 56–66